Local electronic structure of Cu-doped GaN investigated by XANES and x-ray linear dichrosim

R. Schuber,[1,*] P. R. Ganz,[1] F. Wilhelm,[2] A. Rogalev,[2] and D. M. Schaadt[1]
[1]*Institute of Applied Physics/DFG-Center for Functional Nanostructures (CFN), Karlsruhe Institute of Technology, DE-76131 Karlsruhe, Germany*
[2]*European Synchrotron Radiation Facility (ESRF), FR-38043 Grenoble Cedex, France*
(Received 8 June 2011; published 18 October 2011)

X-ray absorption near edge structure (XANES) and x-ray linear dichroism (XLD) measurements of a series of Cu-doped GaN samples with different doping concentrations were investigated at the Ga and Cu *K* edges to get insight into the preferred occupation site of Cu in the GaN matrix. The XLD data of the Cu *K* edge clearly demonstrates that Cu is incorporated in the GaN film. γ-Cu_9Ga_4 compounds that formed on the samples during the GaN growth process could be partially removed by etching with HNO_3. At both absorption edges, a clear increase of the XLD signal intensity could be observed after etching as a consequence of the removal of the γ-Cu_9Ga_4 compounds. By performing simulations of XANES and XLD spectra, which are compared to the experimental data, it was possible to show that most Cu in the GaN film is incorporated on Ga or interstitial sites and only a minor fraction on N sites.

DOI: 10.1103/PhysRevB.84.155206 PACS number(s): 61.72.U−, 61.05.cj

I. INTRODUCTION

Cu-doped group III nitrides have recently earned great interest due to the experimental evidence of ferromagnetism observed in GaN:Cu (Ref. 1) and AlN:Cu (Ref. 2) at room temperature. The usage of Cu as a dopant, which is a nonmagnetic element, excludes the possibility of magnetic clusters built by the dopant. Therefore, the occurrence of ferromagnetism in GaN:Cu does not originate from either Cu or GaN, but is a result of the interaction between the host material and the dopant.

Theoretical work studying ferromagnetic Cu-doped GaN has foremost assumed Cu atoms on substitutional Ga sites, for example.[3–6] For instance, Wu *et al.*[3] explain that incorporation scenarios other than Cu substituting Ga sites are not taken into account because they are energetically unfavored. However, since most growth processes of doped GaN do not take place in an equilibrium environment, the occupation of unfavorable energetic states may not be excluded. Seong *et al.*,[7] stating ferromagnetism in Cu-doped GaN nanowires, show by anomalous x-ray scattering that Cu atoms do indeed substitute onto Ga sites, but do not comment on nitrogen or interstitial site occupation. It is still unclear as to what extent Ga sites are occupied and whether N or interstitial sites also play a role in Cu incorporation. Because the microscopic mechanism of this system's ferromagnetism is still not fully understood, it is of particular interest to clarify the basic question of the positioning of Cu in the GaN matrix.

For this purpose, x-ray absorption near edge structure (XANES) and x-ray linear dichroism (XLD) measurements of a series of Cu-doped GaN samples with different doping concentrations were investigated at the Ga and Cu *K* edges. While in XANES, the edge position and shape is sensitive to the formal valence state, ligand type, and coordination environment, which can be used to identify phases,[8] XLD provides a convenient tool to probe the local structural and electronic properties of the Cu atoms in the nitride host since it is proportional to the anisotropic unoccupied density of charge.[9] The XLD spectrum is therefore highly sensitive to the local symmetry and gives a unique signature in the case of wurtzite structure and no signal amplitude for cubic crystal symmetry.[9] By comparing the measured data to simulations performed by use of the FDMNES code,[10] we find that Cu atoms are incorporated in the nitride host mostly as Ga substitutes and interstitials and to a minority fraction on N sites.

In this paper, we first describe the experimental procedure of the sample preparation, measurements at the synchrotron in Grenoble, and details to the simulations. Thereafter, the results of a surface analysis of the samples will be discussed followed by the presentation of the XLD and XANES data, which are then interpreted with help of the calculated spectra.

II. EXPERIMENTAL PROCEDURE

The investigated samples were grown at the Karlsruhe Institute of Technology by plasma-assisted molecular beam epitaxy. A series of six GaN:Cu samples with varying nominal Cu concentration from 0% to 2.69%, in the following labeled A (0%), B (0.50%), C (1.35%), D (1.77%), E (2.22%), and F (2.69%), were produced. The term nominal concentration used here refers to the flux ratio of Cu atoms to the total metal-atom flux of Cu and Ga. Assuming sticking and incorporation coefficients to be the same for Cu and Ga and equal to unity, these numbers would represent an estimate of the actual doping concentration of Cu. However, these assumptions are not justified and, hence, the nominal concentration can only be seen as a measure of the relative flux provided during growth. As will be described later, a significant part of the provided Cu atoms form metal compounds in the samples, i.e., not all of the provided Cu is available as doping material in the GaN film. In this series of samples, sample C with 1.35% nominal Cu doping takes in a special position due to the measured ferromagnetic behavior. The data are not shown here, but their magnetic behavior as well as the growth procedure applied is very similar to the case reported earlier.[11] It may be remarked that the ferromagnetic sample C shows no discrepancy in the magnetic data between the as-grown and etched parts of the sample, where the metal compounds had been removed; we therefore see no connection between the metal-compound formation and the sample's magnetic behavior.

 ©2011 American Physical Society

To obtain better thermal coupling during growth, *C*-plane-oriented sapphire substrates were mounted onto silicon using indium as an adhesive. Each substrate was first outgassed in a baking chamber at 130 °C for 60 min before introducing it into the growth chamber. It was then heated to 890 °C for 30 min for a final outgassing step before nitridation commenced for 180 min at 200 °C. A thin AlN buffer layer [thickness $\approx 22 \pm 4$ nm as measured by scanning electron microscopy (SEM)] was introduced prior to the growth of the epitaxial Cu-doped GaN layer. A growth rate of roughly 70 nm/h was used, resulting in GaN film thicknesses in the range of 130–150 nm. After unloading the sample from the molecular beam epitaxy system, it was cut into parts, one of which was etched and one left unetched. The etching of the samples was performed to remove metal compounds from the samples and included 65% HNO_3 treatment for 5 min and rinsing with deionized water. To obtain an understanding of the effect of etching on the samples, their surfaces were investigated by SEM.

For all samples, the XANES and the XLD spectra were measured at the *K* edges of Ga and Cu, i.e., around 10 367 eV and 8979 eV, respectively. These measurements were performed with hard x-rays from the ID12 beamline at the European Synchrotron Radiation Facility (ESRF) detecting the total fluorescence yield. The experimental chamber contains eight silicon photodiodes arranged in a semisphere around the sample that are equipped with 10-μm-thick Ni filters. A quarter wave plate was used to flip the linear polarization of the synchrotron light from vertical to horizontal when performing the XLD measurements, also described in detail in Ref. 12. The angle of incidence was between 14° and 17° with respect to the sample surface. For the analysis of the XANES and XLD spectra, we have to keep in mind that the illuminated sample area is much larger than the size of a surface compound and also much larger than the mean distance between the compounds. The x-ray signals collected are therefore an average of the sample and do not probe parts of the sample locally. In addition, the hard x-rays of the synchrotron are assumed to penetrate the samples completely, leading to a probing of the whole volume of the samples instead of only the surface layers.

XANES and XLD spectra were simulated using the FDMNES code[10] applying the multiple scattering formalism within the muffin-tin approximation. To obtain a doping concentration of Cu in GaN, which is comparable with the Cu concentration in the experimental samples, a wurtzite supercell of $4 \times 4 \times 4$, i.e. a total of 256 atoms, with a calculation radius of 10 Å, was used. GaN lattice constants of $a = 3.188$ Å and $c = 5.185$ Å were used.[13] For the x-ray absorption spectra, eight different doping concentrations were calculated, the lowest possible ranging from 0.78% (with 1 Cu atom in the supercell) up to 6.25%. The variation of doping concentration in the supercell, however, has almost no influence on the calculated spectra. Due to this fact, for reasons of clarity, only the 1.56% doped spectra are plotted in the analysis to follow. Configurations of Cu in the GaN crystal substituting Ga atoms, N atoms, or as interstitials in the largest void of the GaN matrix (see Fig. 1) were performed. The two Cu atoms are separated by the largest possible distance to avoid possible clustering effects.

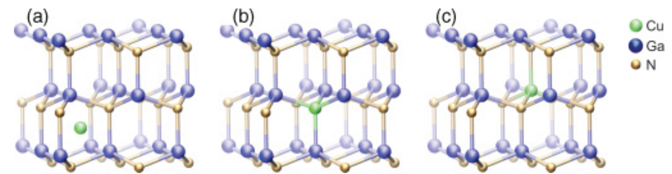

FIG. 1. (Color online) Schematic representation of part of a GaN $4 \times 4 \times 4$ supercell. (a), (b), and (c) show how the Cu atoms are placed in the GaN matrix on interstitial, N, and Ga sites, respectively.

III. RESULTS AND CONCLUSION

During growth of the Cu-doped GaN samples, Cu is not only incorporated in the film but also forms cubic,[14] nonmagnetic γ-Cu_9Ga_4 structures according to x-ray diffraction[1] (XRD) and transmission electron microscopy (TEM) analysis.[15] As pointed out in Ref. 15 regarding the phase diagram of Ga-Cu-N compounds, it is difficult to completely avoid γ-Cu_9Ga_4 formation in the growth process. However, work is currently underway to explore other growth regimes where an enhanced incorporation of Cu in GaN, simultaneously decreasing the synthesis of γ-Cu_9Ga_4, is expected. Because a complete lack of γ-Cu_9Ga_4 in the samples is presently unavailable, there are different placement possibilities of the Cu atoms in the sample (in the GaN film or in the γ-Cu_9Ga_4 structures) and, hence, a clear distinction of the origin of the Cu signals present in the XANES and XLD spectra must be clarified. For this purpose, measurements on as-grown samples as well as on samples where the surface compounds had been removed by wet chemical etching were compared.

In a first step, an estimate of the Cu incorporation in the GaN film and the γ-Cu_9Ga_4 compounds is done by means of SEM surface analysis. This gives a better understanding for the following analysis because the intensity of the absorption signal is proportional to the amount of atoms present in a specific chemical configuration. Since XLD probes the anisotropy of the valence charge, Cu atoms in GaN give a wurtzite-type signature if, e.g. substituting Ga sites, but should give no signal contribution when bound in γ-Cu_9Ga_4 compounds as a result of the compounds' cubic symmetry.[16] In a second step, the x-ray absorption spectra are examined.

From the surface-sensitive SEM analysis, the majority of Cu, which is incorporated in the sample, is expected to be found in the γ-Cu_9Ga_4 compounds. This observation is still valid after etching, where most of the γ-Cu_9Ga_4 could be removed, however, leaving behind between 12% and 35% of the compounds, depending on the sample. Due to the expected big influence of γ-Cu_9Ga_4 compounds on the absorption spectra, we first turn to look at the XLD spectra, where only a noncubic coordination of Cu gives a nonzero signal, to make sure Cu is really incorporated in the GaN film. We shall see in the following that we do indeed observe a nonzero XLD signal at the Cu *K* edge, proving Cu occupation in the GaN crystal. To gain confidence to the answer of the actual Cu placement in GaN, we thereafter analyze the XANES spectra, which are not dominated by the Cu signal incorporated in GaN, but are surely influenced by it. XANES and XLD simulations of Cu-doped GaN, performed for Cu placement on Ga, N, and interstitial sites and of γ-Cu_9Ga_4 compounds, are compared

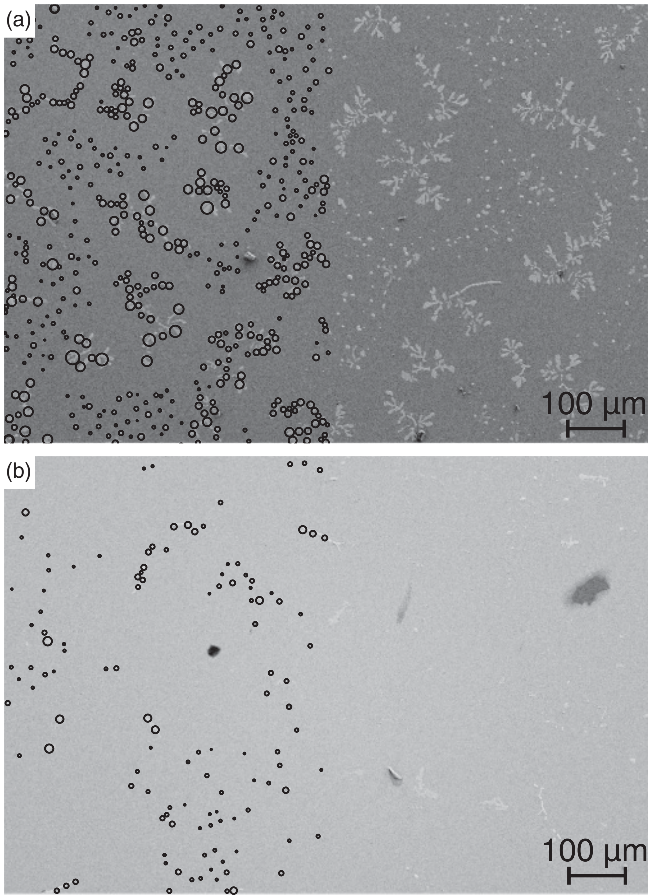

FIG. 2. SEM image of sample F (2.69%) before etching (a) and after etching (b). On the left sides of the pictures, the surface coverage of the precipitates is estimated by approximating the structures' area with the area of multiple small circles. For this sample, a 88% decrease in the surface coverage of the surface structures is calculated from the pre-etched to the post-etched condition of the sample.

to the experimental data to extract numbers for the fractions of differently occupied sites in GaN by Cu.

A. γ-Cu_9Ga_4 surface compounds

A first estimate for the amount of Cu present in the surface compounds (γ-Cu_9Ga_4) with respect to the film can be deduced estimating the γ-Cu_9Ga_4 island coverage using SEM images (Fig. 2) and an average height estimate of 220 nm from TEM pictures of the samples.[15] An important assumption included in the following evaluation, namely, that all the precipitates visible on the sample surfaces are only composed of γ-Cu_9Ga_4, is justified by the fact that they are all formed during growth, i.e. at a temperature of 790 °C (by thermocouple reading). This can be assumed because some of the compounds have been overgrown by a thin GaN film and are supported by TEM data.[15] Further, a mean Cu to Ga ratio with 32.78% Ga in these compounds is assumed in accordance with the phase diagram given in Refs. 17 and 18.

A decrease in surface compounds on the samples could be achieved by etching. This is clearly seen for sample F in SEM images taken of the as-grown [Fig. 2(a)] and the etched [Fig. 2(b)] samples. The left part of the pictures, where black circles surround the structures, is an example of how the estimated surface coverage of γ-Cu_9Ga_4 was taken into account in the calculations (in this case, the area covered by γ-Cu_9Ga_4 was 8.22% of the total sample area). The sample after etching showed an 88% decrease of the compounds. Table I gives an overview of all the Cu-doped samples with their nominal Cu concentration, and in each case, the values of the volume percentage of γ-Cu_9Ga_4 in the sample before and after etching along with the relative and absolute decrease of the amount of compounds. The last two columns give the calculated ratio of Cu atoms bound in the compounds with respect to the total metal-atom content of the sample (excluding the amount of Cu in the film, as it is known only for sample C). The fact that the amount and size of the γ-Cu_9Ga_4 compounds on the sample surface increases with increasing nominal Cu concentration is clearly reflected in the numbers of Table I.

Note that the calculated ratio of Cu, forming compounds, to the total metal content is already higher than the provided Cu to metal flux ratio during growth. This is a plausible outcome because the provided flux ratio of Cu and Ga is not the same ratio as is built into the sample. It is a clear indication that the sticking and incorporation coefficients of Cu and Ga on GaN are different. While the sticking coefficient for Cu can be assumed to be near unity because of its low vapor pressure at the growth temperature used in this study,[19,20] it is higher for Ga.[21] It is therefore impossible to deduce a reliable number for the Cu concentration in the GaN film by this kind of analysis. However, using results obtained by wavelength dispersive x-ray spectroscopy (WDXS) on a 1.38% nominally Cu-doped sample, where 0.26% of the metal atoms in the GaN film were Cu atoms,[15] we can deduce a real doping of 0.24% Cu for sample C assuming the same Cu incorporation rate for both these samples. This means that, considering the presence of γ-Cu_9Ga_4 compounds, approximately 3.1% of the Cu atoms

TABLE I. Listing of the Cu-doped GaN samples with the estimated γ-Cu_9Ga_4 coverage by SEM measurements.

	Nominal conc.	$V_{Cu_9Ga_4}/V_{sample}$ (%)		$V_{Cu_9Ga_4}$ decrease	$V_{Cu_9Ga_4}$ decrease	# Cu at. in γ-Cu_9Ga_4/ # metal at. [%]	
Sample	(%)	Unetched	Etched	(%)	(mm^3)	Unetched	Etched
B	0.50	1.46	N.a.			3.47	
C	1.35	3.19	0.81	79.74	3.47×10^{-4}	7.26	1.95
D	1.77	5.72	3.02	65.43	4.13×10^{-4}	12.27	6.89
E	2.22	6.39	2.15	74.84	6.48×10^{-4}	13.51	5.01
F	2.69	11.44	1.56	88.03	15.88×10^{-4}	21.78	3.68

FIG. 3. (Color online) The measured XLD spectra depicted here were normalized to the background at the lowest and the highest energies of the spectrum. (a) and (b) are the XLD spectra of the Ga K edge prior to and after etching of the samples, respectively. (c) and (d) show the XLD spectra of the Cu K edge before and after etching of the samples, respectively. Bragg peaks are marked by "×".

in the sample are incorporated into the GaN film, whereas the remaining roughly 96.9% are found in the compounds. The situation appears reversed when calculating the percentage of Ga in the film and in the compounds, where the estimated numbers are 96.5% and 3.5%, respectively.

As a first outcome of these estimates, we can state that the majority of Cu that is present in the samples is incorporated in the compound of γ-Cu_9Ga_4. By etching, it was possible to remove most of the compounds, but not to 100%. The XANES spectra are therefore expected to be dominated by signals originating from the compounds. XLD, however, is insensitive to cubic coordination of bound atoms and shall therefore be free of a signal originating from the γ-Cu_9Ga_4 compounds. In the following, the analysis of XLD at the Ga K edge followed by the Cu K edge will be shown. Thereafter, the XANES spectra at both edges will be discussed.

B. X-ray linear dichroism of Cu-doped GaN

1. *XLD at the Ga K edge*

In XLD spectra recorded for the etched and unetched samples at the Ga [Figs. 3(a) and 3(b)] and Cu K edges [Figs. 3(c) and 3(d)], we can clearly see an increase of the XLD signal for the etched samples compared to the unetched ones. Regarding the Ga edge, the increase of signal amounts to an average of about 7% to 33%, depending on the sample. This

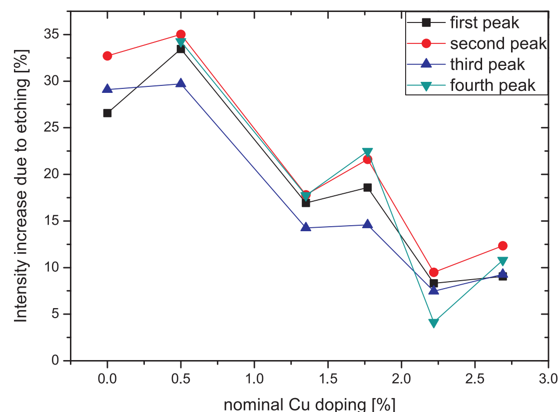

FIG. 4. (Color online) The intensity increase of the XLD peaks at the Ga K edge between etched and unetched samples is shown as a function of the nominal doping concentration. The increase is due to the removal of γ-Cu_9Ga_4 compounds (see text for discussion).

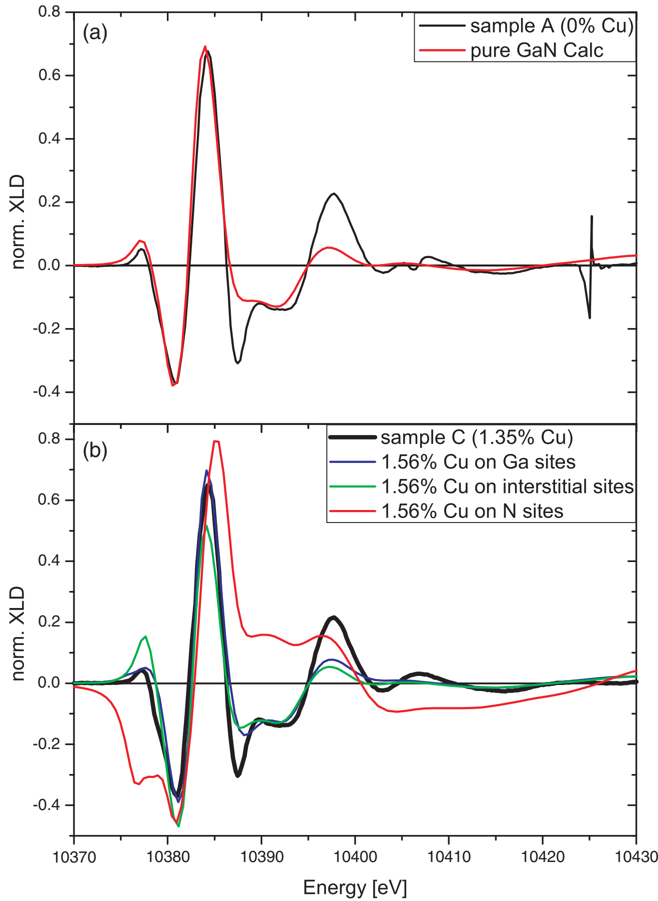

FIG. 5. (Color online) Comparison of the measured Ga K-edge XLD signal to the simulated ones. (a) shows the undoped spectra, while (b) displays the measured graph of sample C (1.35%) in comparison to calculated spectra for different Cu site possibilities.

behavior of the XLD signals' intensity increase due to etching for the different samples and peaks can be seen in Fig. 4. The intensity variation between etched and unetched samples can be explained by the fact that, after etching, cubic surface compounds (γ-Cu_9Ga_4) have been removed and a higher percentage of the signal collected origins from the wurtzite film, hence giving more intense peaks in the XLD spectrum. The nonuniformity in the increase of the intensity can be ascribed to the different amount of compounds removed from the different samples, as was also seen in the SEM analysis above (see the absolute $V_{Cu_9Ga_4}$ decrease column in Table I). The tendency of higher nominally doped samples giving less increase of the XLD signal is presumably due to the short etching time applied. This means that because more Cu supply during growth leads to more compounds, a longer etching time is needed to completely remove the compounds. However, for all samples, the etching time was constant, leading only to a partial removal of the compounds and in conclusion to a higher percentage of remaining γ-Cu_9Ga_4 on the samples having been exposed to higher Cu fluxes.

The sharp Bragg peaks in the graphs of Fig. 3 are marked by "×" and occur because some crystal lattice planes in the samples satisfied the Bragg condition with respect to the position of some of the detectors and yield no information which is of interest here. Apart from the slight variation in intensity, an examination of differences in the Ga K-edge XLD signal in dependence of the Cu doping can not be observed. However, comparing the experimental XLD data of the Ga K edge to simulations [Fig. 5(b)], we can state that only a very small percentage of Cu atoms is located on N substitutional sites. This conclusion is drawn from the qualitatively greatly differing curve progression of the simulated data for 2 N atoms having been replaced by 2 Cu atoms in a $4 \times 4 \times 4$ supercell calculation. A clear analysis of a quantitative measure of Cu atoms occupying Ga, N, or interstitial sites is not possible at this stage due to the inaccuracy in modeling these spectra. The effect of the inaccuracy can be shown in Fig. 5(a) where the experimental and simulated data of pure GaN are depicted. Although a fairly good qualitative agreement is apparent, it shows that the fit is not good enough to discriminate between Cu on Ga or interstitial sites in Fig. 5(b).

2. XLD at the Cu K edge

The much lower signal-to-noise ratio of the XLD signals of the samples recorded at the Cu K edge compared to the Ga edge data is clearly visible in Figs. 3(c) and 3(d). Nevertheless, the increase of the signal from the unetched to the etched samples is apparent, again resulting from a lower fraction of compounds present in the samples, thereby being responsible for less absorption of x-rays in the cubic structure (not contributing to the XLD signal). In Fig. 3(c), sample B seems to divert significantly from the rest of the samples. This is, however, not considered to be of physical origin; rather, the behavior is traced back to difficulties in reliably normalizing the data acquired for this sample due to the presence of two intense Bragg peaks (marked by "×" in the graph) and the low statistics compared to the data of the other samples, therefore being responsible for impracticable intensity comparisons. Due to the generally low statistics of the data for all samples, resulting from limited beam time and a low incorporation amount of Cu in the GaN film, a comparison of the signals' intensities with respect to the different doping concentration is unfeasible. However, a clear statement of the presence of an XLD signal is possible, leading to the conclusion that Cu is really incorporated in the GaN film and is not merely present in the form of γ-Cu_9Ga_4 compounds.

Although the statistics of the experimental data makes a quantitative analysis difficult, an idea of where most of the Cu atoms are placed in the GaN host lattice can be extracted when comparing the nonzero XLD measured signal to the simulations (Fig. 6). We observe that the intense first negative peak in the Cu on N sites graph is missing in the experimental data. Hence, a large percentage of Cu on N sites can safely be assumed to be limited to a very small amount. Similarly, the Cu on Ga and interstitial sites make a contribution to this first negative peak, but with much lower intensity, therefore, not contradicting with the possibility of a significant percentage of these configurations being present but unresolved in the experimental data. Interestingly, the best matching spectra to the experimental curve is the XLD signature of Cu on interstitial sites where the shape of the maxima correspond well with the two peaks in Fig. 6(d).

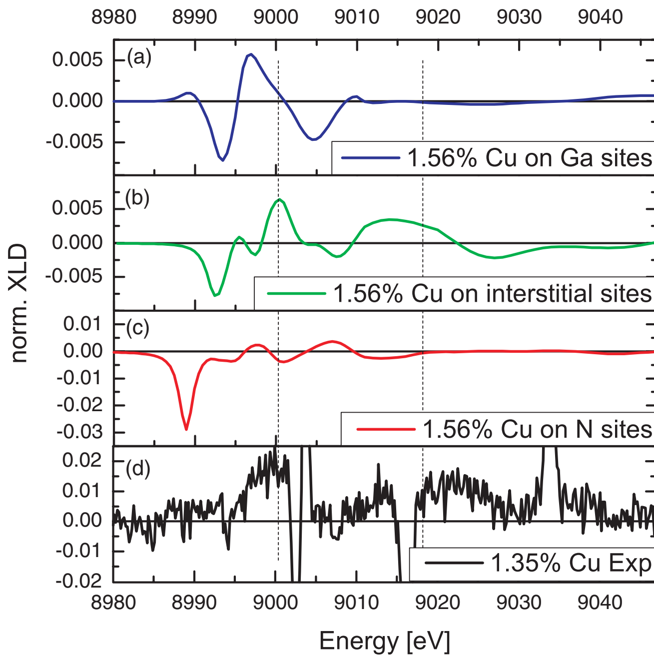

FIG. 6. (Color online) (a)–(c) depict the Cu K-edge XLD simulation results for 1.56% Cu-doped GaN on Ga, N, and interstitial sites, (d) shows the experimental data of sample C (1.35%). As a guide to the eye, the two main peaks present in (d) are marked by dotted lines throughout the other graphs.

C. X-ray absorption near edge structure of Cu-doped GaN

1. *XANES at the Ga K edge*

The experimental XANES data of the samples at the Ga K edge [Fig. 7(a)] show hardly any variation for the different doping concentrations. This is expected because the amount of Cu incorporated in the lattice is small leading to even smaller differences in the incorporation amount from one sample to another, which should not affect the Ga signal of the film a great deal. The large spikes in the higher energy region of samples A (0.00%), B (0.50%), and D (1.77%), marked by "×" in the graph, are again Bragg peaks that are only avoidable when tilting the sample. Here, however, the peaks are well away from the region of interest in the spectrum, thereby not causing any confusion identifying the real XANES signal.

In Fig. 7(b), the comparison of one of the experimental curves (sample C) with the simulated data is shown. Here, simulation results are shown for pure wurtzite GaN (0% Cu) as well as for GaN with 2 Cu atoms in a $4 \times 4 \times 4$ supercell (1.56% Cu) replacing Ga atoms, N atoms, and situated as interstitials.

The comparison of the calculated data with the experimental data in Fig. 7(b) displays general agreement between the two in a number of points. The main peak around 10 383 eV is very well described by all simulated curves apart from the curve for Cu on N sites, which is shifted to higher energies by 2 eV. One might be tempted to explain the high-energy shoulder of the main peak by a possible admixture of Cu occupation of N sites in GaN. This case is repeated for the next peak at around 10 395 eV, where again the high-energy shoulder in the experimental data could be explained by the substitutions of Cu on N sites. However, as these shoulder peaks in the experimental spectrum are also present in the undoped GaN spectrum, we no longer need to analyze the origin of these features with respect to Cu doping. We assume that the lack of precise matching comes about because of the inaccuracy of the theory and claim that the low percentage of Cu in the GaN film does not noticeably affect the spectrum. Further, the simulations fail to describe more details of the measurement, most noticeably the low-energy rising edge of the spectrum where a distinct peak in the experimental data is seen. This peak also appears in the calculations but is rather a shoulder. It is most pronounced when Cu occupies interstitial sites in the GaN lattice; its exact origin, however, can not be concluded to be due to Cu, for the same argument as above holds, namely, that it is also present in the undoped sample. Ga bound in γ-Cu_9Ga_4 compounds can not be seen to influence the spectrum as the double-peak feature in the calculated γ-Cu_9Ga_4 spectrum is completely absent in the experimental data. The calculation of γ-Cu_9Ga_4 was performed for one unit cell (52 atoms) and a cluster calculation radius of 10 Å.

2. *XANES at the Cu K edge*

Turning to the XANES spectra at the Cu K edge [Fig. 7(c)], as in the case for the Ga K edge, there is no significant difference visible between the samples with different Cu concentrations. This outcome is not surprising, remembering the considerations above, involving the SEM images, where we stated that other than for the Ga signal, the Cu signal mainly has its origin from the Cu incorporated in the γ-Cu_9Ga_4 compounds and not from Cu in the GaN film. The spectrum of sample B may seem to differ from the rest, but with regard to the lower statistics in the experimental data for this sample compared to the others, also apparent in the lower signal to noise ratio, the small deviation to the rest of the samples can be considered insignificant.

Figure 7(d) depicts the experimental data as well as the simulated data for 1.56% Cu-doped GaN where Cu is sitting on Ga or N substitutional sites as interstitials or is bound in γ-Cu_9Ga_4. It can clearly be seen that the shape of the experimental data most accurately fits the calculated γ-Cu_9Ga_4 graph. However, the shoulder in the rising edge of the measured data is not accounted for in the γ-Cu_9Ga_4 curve. This aspect can be explained by a slight portion of N sites being occupied by Cu atoms. Unfortunately, as can be seen by the strongly γ-Cu_9Ga_4 dominated shape of the experimental data, signals of an admixture of the Cu component coming from the Cu atoms incorporated in the GaN film are highly suppressed, i.e., an experimental curve fit with a contribution of one or more of the GaN:Cu curves can be established, but is subject to a large uncertainty.

Although an accurate fit is not possible for the entire spectrum, a tendency of Cu site occupation can be extracted when deconvoluting the XANES Cu K-edge spectrum (Fig. 8) by considering the four possible signal origins (Cu on Ga, N, interstitial sites, or in γ-Cu_9Ga_4). A good overall fit of the experimental data was achieved for a placement of Cu atoms at 4.0% Ga, 0.6% N, and 1.1% interstitial sites; the remaining 94.3% of the signal is attributed to γ-Cu_9Ga_4. This means that for Cu in the film, 70% is on Ga, 20% on interstitial, and 10% on N sites. Although these numbers are values for the best

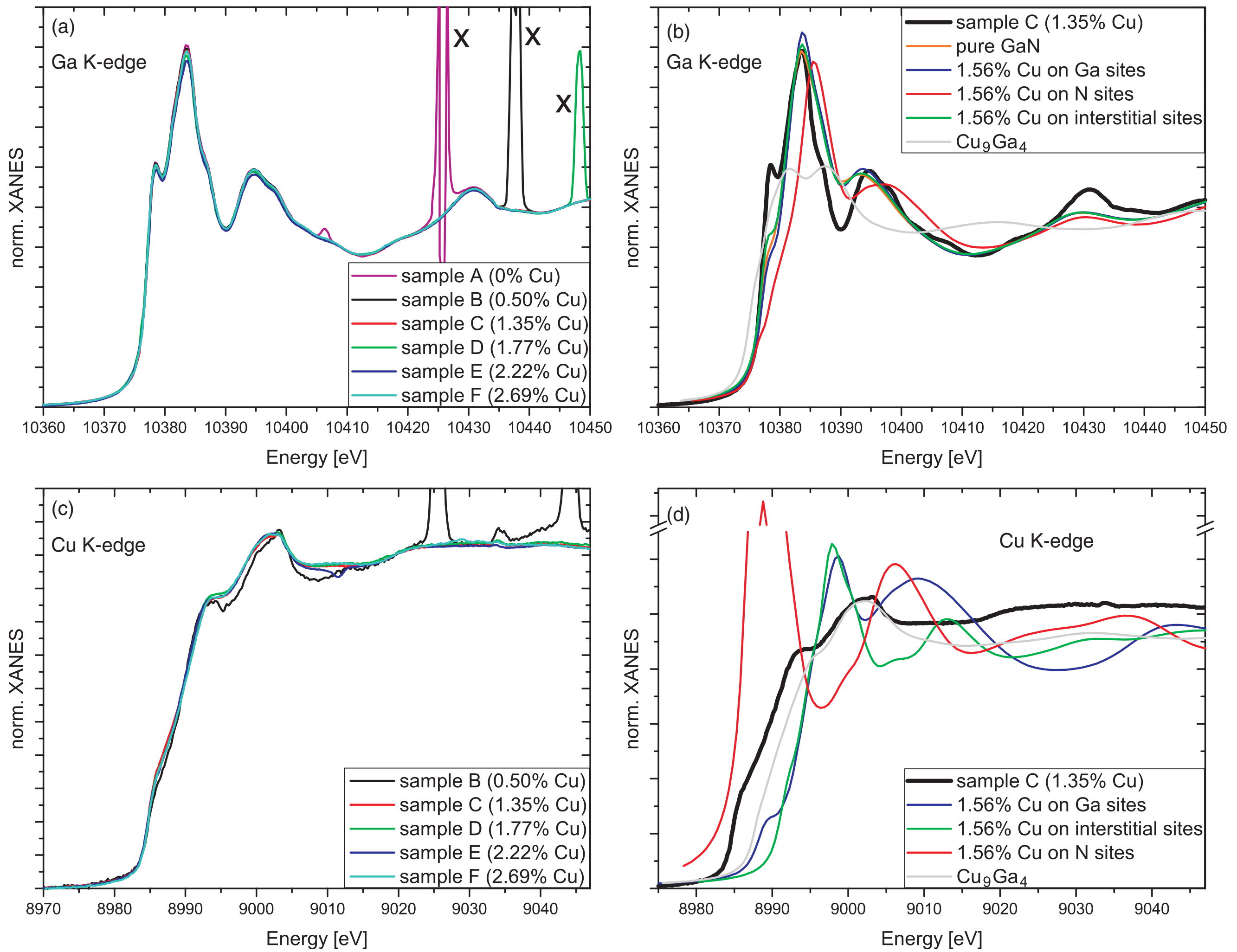

FIG. 7. (Color online) Experimental XANES spectra of the Ga (a) and Cu (c) K edge for the differently doped samples. (b) and (d) show the experimental XANES data of sample C (1.35%) along with calculated spectra for Cu on different sites for the Ga and Cu K edges, respectively.

fit when deconvoluting the experimental spectrum, the error bars are rather large, i.e., similar fits can be obtained with a different occupation of Cu in GaN. To find a range where this is possible, the data were fit with the maximum tolerable Cu fraction in each position of Cu on Ga, N, and interstitial sites. The result is that Cu can occupy between 0%–6.2% Ga, 0%–0.8% N, and 0%–6.8% interstitial sites in GaN within the sensitivity of our measurement and is to 93.2%–100% present in γ-Cu_9Ga_4 compounds.

Going back to the simulation of XLD spectra at the Cu edge and plugging in the values of Cu occupation on the different GaN sites extracted from XANES, we expect to see a good fit with the experimental data if the XANES fit was reasonable. The simulation, where the composition of the signal is the same as the one determined by the XANES data, and the experimental data are shown in Figs. 9(a) and 9(b), respectively. It can be seen that the calculation describes the measured XLD data well within the sensitivity of the measurement. Further, the order of magnitude of the signal's intensity is well described in this case where the majority of the signal is assumed to be absorbed by the γ-Cu_9Ga_4 compounds. The fact that the fit results of the XANES spectra correspond well to the XLD spectra is an important check for consistency and makes the data, in spite of the low signal-to-noise ratio, reliable.

The results from this analysis roughly correspond to the results from the SEM considerations above, i.e., from XANES we conclude that 5.7% of the Cu in the sample is in the film, whereas from a combined SEM and WDXS analysis, it was an estimated fraction of 3.1%. Due to the numerous assumptions leading to these numbers, the discrepancy is not surprising. Nevertheless, important information can be gained: Cu is incorporated in the film; Cu is not only incorporated on Ga sites; Cu occupies N sites to a measurable extent. This is a finding that has not been previously reported and may lead to new theoretical considerations of different defects, other than only Cu substitutions on Ga sites.

D. Considering strain in γ-Cu_9Ga_4 compounds

TEM investigations have revealed epitaxial growth of γ-Cu_9Ga_4 compounds on GaN (Ref. 15), which indicates the

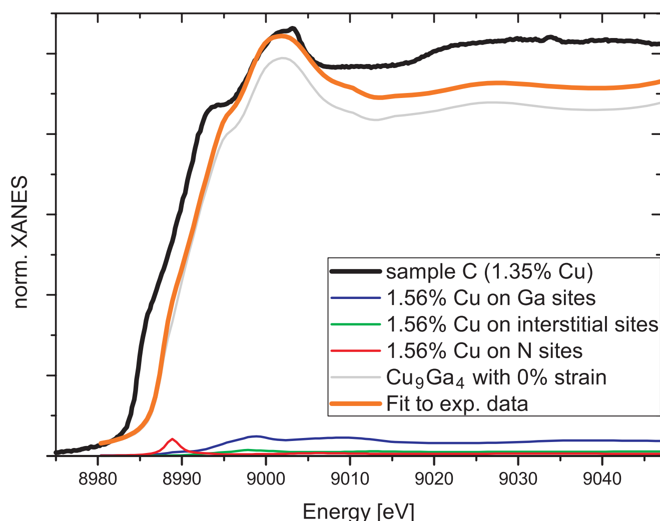

FIG. 8. (Color online) Fitting of the experimental XANES graph of sample C (1.35%) with different calculated Cu site positions.

possibility of γ-Cu_9Ga_4 being strained and thereby deviating from its cubic structure. This means that strained γ-Cu_9Ga_4 could also be responsible for the XLD signal that has been observed. Therefore, XANES and XLD spectra of strained γ-Cu_9Ga_4 are also investigated. Different magnitudes of biaxial compressive strain have been considered ranging from 0.5% to 20%.

A change in the γ-Cu_9Ga_4 structure is expected to influence the XANES spectrum at the Cu edge. Indeed, the shape of the graph and the main peak position changes with varying strain. Best agreement to the measured data is given in the range of 13%–15% strain, which is a significant amount of strain and should be experimentally observable by, e.g. XRD. However, XRD as well as in TEM measurements, where such a large strain of the compounds should be visible, show no indication of strain in the compounds within the measurement sensitivity.

A further indication that a contribution of strained γ-Cu_9Ga_4 to the spectra is highly improbable is the increase of the XLD signal for the etched samples compared to the unetched ones, which has been discussed above and is depicted in Fig. 4. If strained γ-Cu_9Ga_4 were responsible for a large part of the XLD signal, a decrease (rather than an increase) of XLD signal intensity after etching, due to partial removal of the γ-Cu_9Ga_4 compounds, would be expected.

In addition to these arguments, XLD spectra of simulations were performed for up to 20% strained γ-Cu_9Ga_4 to get an estimate of the influence on the XLD spectra of strained γ-Cu_9Ga_4. The results are shown in Figs. 10(a) and 10(c) together with the experimental data of sample C [Fig. 10(b)] for comparison. None of the calculated spectra are in good agreement with the experimental curve and, hence, the possibility of strained γ-Cu_9Ga_4, also from this viewpoint, is very small.

All these observations show that the presence of strain in γ-Cu_9Ga_4, due to epitaxial growth on GaN, is negligible for the analysis of the presented data. However, in order to estimate the sensitivity of the fit presented in Fig. 8 on the shape of the simulated γ-Cu_9Ga_4 spectrum, the experimental XANES spectrum at the Cu edge was fitted. Figure 11 shows this fit considering 14% biaxial compressive strained γ-Cu_9Ga_4. The

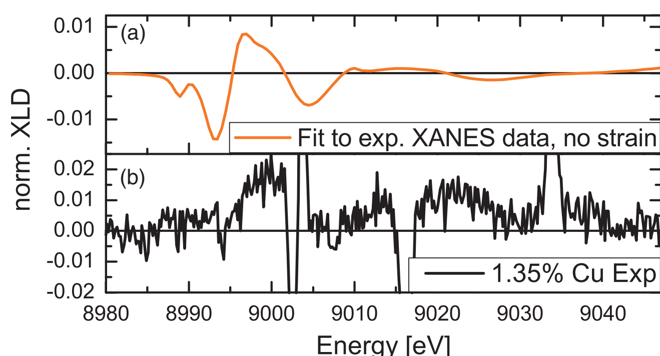

FIG. 9. (Color online) (a) shows the simulated XLD data of GaN:Cu with a mixture of the possible sites (Ga, N, interstitial) that Cu can occupy, according to the same fractions of contributions as described for the XANES spectra in Fig. 8. (b) displays the experimental XLD curve of sample C.

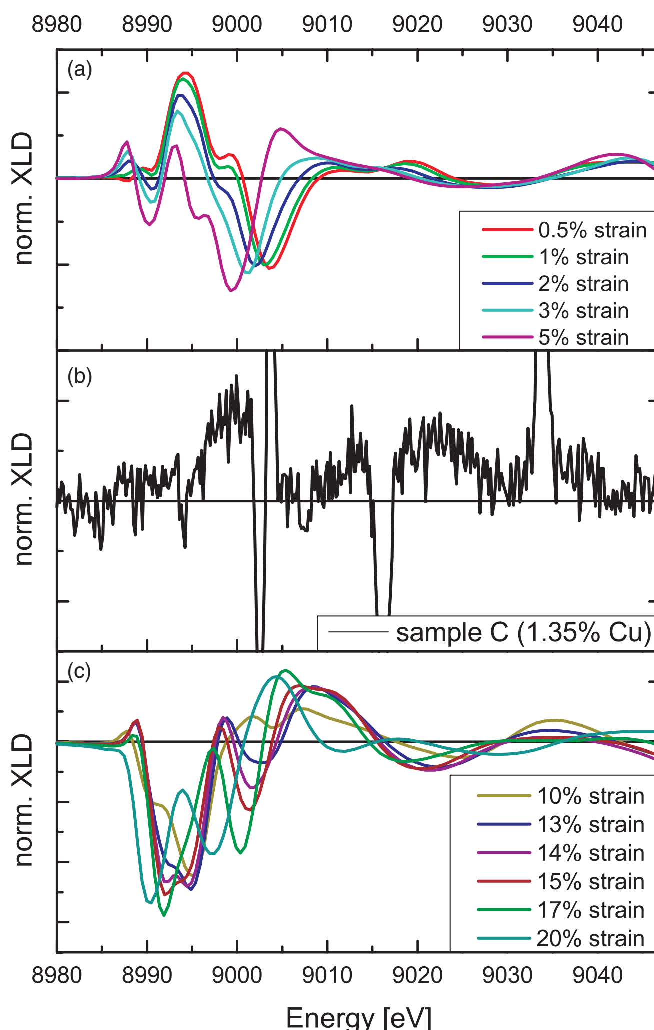

FIG. 10. (Color online) Comparison of the XLD signals of strained γ-Cu_9Ga_4 (a) and (c) and the experimental curve (b) of sample C (1.35%) at the Cu K edge. None of the calculated spectra correspond well with the experimental one, indicating the absence of strain in γ-Cu_9Ga_4.

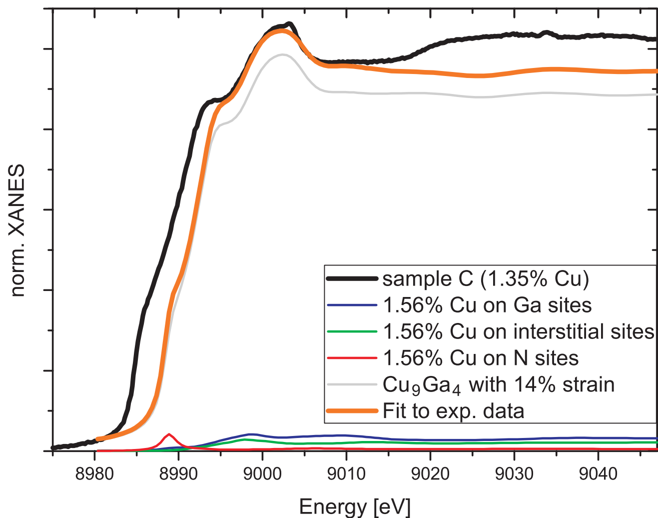

FIG. 11. (Color online) Fitting of the experimental XANES graph of sample C (1.35%) with different Cu site positions, where the γ-Cu_9Ga_4 compounds are subject to 15% biaxial compressive strain.

change in Cu occupation distribution, with the best fit value given in brackets, is as follows: 0%–10.6% (3.3%) for Cu on Ga, 0%–0.5% (0.5%) for Cu on N, 0%–7.7% (2.2%) for Cu on interstitial sites, and 89.4%–100% (93.9%) for Cu in metal compounds. Regarding Cu in the film only, this means that 54.5% is on Ga, 36.4% on interstitial, and 9.1% on N sites. Introducing strain to the compound, the difference of Ga or interstitial site occupation plays a less important role for the shape of the graph.

Comparing the fitting results of the strained and unstrained scenarios (Figs. 8 and 11), we find that in both cases, mostly Ga positions are occupied by Cu, followed by interstitials and about 10% are present in N-like coordination. The values for Ga and interstitial site occupation are subject to a rather large error; however, because of the greatly differing shape of the spectrum for Cu atoms on N sites, this value is consistent in both scenarios.

IV. SUMMARY

A series of etched and unetched Cu-doped GaN samples with different doping concentrations have been investigated by XANES and XLD measurements to evaluate where Cu atoms are incorporated in the GaN matrix. The observed XLD signal at the Cu K edge proves the incorporation of Cu in GaN and indicates that mainly Ga and interstitial positions in GaN are occupied by Cu. The XANES spectra at the Cu K edge are dominated by the signal coming from γ-Cu_9Ga_4 compounds. With the knowledge that the XANES spectra must also be affected by Cu present in GaN, a fit of the experimental XANES data was performed, taking into account a possible placement of Cu in the GaN crystal on Ga, N, and interstitial sites. The findings show that a large majority of the Cu atoms (∼70%) take Ga substitutional sites, about 20% can be found on interstitial, and 10% on N sites. XLD simulations of GaN, with a Cu site occupation scenario as extracted with the help of the XANES spectra, compared to the experimental data confirm the results in a consistent way.

A contribution of strained γ-Cu_9Ga_4 to the XLD signal is ruled out by a number of observations. The increase of XLD signal intensity after etching and the mismatch of simulated XLD spectra for strained γ-Cu_9Ga_4 with the experimental data indicate the absence of strain in γ-Cu_9Ga_4. This is also consistent with earlier XRD and TEM results, which found no indication of large strain in the compounds.

ACKNOWLEDGMENTS

We acknowledge the European Synchrotron Radiation Facility for provision of synchrotron radiation facilities. The authors from Karlsruhe acknowledge financial support from the Deutsche Forschungsgemeinschaft (DFG) and the State of Baden-Württemberg through the DFG-Center for Functional Nanostructures (CFN) within subproject A2.7. One of the autors (R.S.) would like to acknowledge M. Bürkle for the fruitful discussions on the simulation results.

[*]Corresponding author: ralf.schuber@kit.edu

[1] P. R. Ganz, G. Fischer, C. Sürgers, and D. M. Schaadt, J. Cryst. Growth **323**, 355 (2010).
[2] F. Y. Ran, M. Subramanian, M. Tanemura, Y. Hayashi, and T. Hihara, Appl. Phys. Lett. **95**, 112111 (2009).
[3] R. Q. Wu, G. W. Peng, L. Liu, Y. P. Feng, Z. G. Huang, and Q. Y. Wu, Appl. Phys. Lett. **89**, 062505 (2006).
[4] A. L. Rosa and R. Ahuja, Appl. Phys. Lett. **91**, 232109 (2007).
[5] B. S. Kang, C. M. Heo, K. K. Lyu, and S. C. Yu, Int. J. Magn. **14**, 114 (2009).
[6] S. C. Lee, J. H. Choi, K. R. Lee, and P. R. Cha, J. Korean Phys. Soc. **55**, 1013 (2009).
[7] H. K. Seong, J. Y. Kim, J. J. Kim, S. C. Lee, S. R. Kim, U. Kim, T. E. Park, and H. J. Choi, Nano Lett. **7**, 3366 (2007).
[8] M. Newville, *Fundamentals of XAFS, Consortium for Advanced Radiation Sources* (University of Chicago, Chicago, 2004).
[9] F. Wilhelm, E. Sarigiannidou, E. Monroy, A. Rogalev, N. Jaouen, H. Mariette, and J. Goulon, AIP Conf. Proc. **879**, 1675 (2007).
[10] Y. Joly, Phys. Rev. B **63**, 125120 (2001).
[11] P. R. Ganz, C. Sürgers, G. Fischer, and D. M. Schaadt, J. Phys.: Conf. Ser. **200**, 062006 (2010).
[12] E. Sarigiannidou, F. Wilhelm, E. Monroy, R. M. Galera, E. Bellet-Amalric, A. Rogalev, J. Goulon, J. Cibert, and H. Mariette, Phys. Rev. B **74**, 041306(R) (2006).
[13] M. Leszczynski, Ha. Teisseyre, T. Suski, I. Grzegory, M. Bockowski, J. Jun, S. Porowski, K. Pakula, J. M. Baranowski, C. T. Foxon, and T. S. Cheng, Appl. Phys. Lett. **69**, 73 (1996).
[14] R. Stokhuyzen, J. K. Brandon, P. C. Chieh, and W. B. Pearson, Acta Crystallogr., Sect. B: Struct. Crystallogr. Cryst. Chem. **30**, 2910 (1974).

[15]T.-H. Huang, P. R. Ganz, L. Chang, and D. M. Schaadt, J. Electrochem. Soc. **158**, H860 (2011).
[16]J. Stöhr and H. C. Siegmann, *Magnetism: From Fundamentals to Nanoscale Dynamics* (Springer, Berlin, 2006).
[17]Springer Materials, The Landholt-Börnstein Database [http://www.springermaterials.com/docs/pdf/10086090_1074.html].
[18]J.-B. Li, L. N. Ji, J. K. Liang, Y. Zhang, J. Luo, C. R. Li, and G. H. Rao, CALPHAD: Comput. Coupling Phase Diagrams Thermochem. **32**, 447 (2008).
[19]H. Hersh, J. Am. Chem. Soc. **75**, 1529 (1953).
[20]H. Hersh, J. Am. Chem. Soc. **75**, 6361 (1953).
[21]C. N. Cochran and L. M. Foster, J. Electrochem. Soc. **109**, 144 (1962).